IET Optoelectronics

Research Article

Single mode semiconductor laser based on coupled cavities of an active ring laser and Fabry Perot

ISSN 1751-8768
Received on 12th May 2017
Revised 11th October 2017
Accepted on 7th November 2017
E-First on 27th November 2017
doi: 10.1049/iet-opt.2017.0062
www.ietdl.org

Mohamad Dernaika[1,2] ✉, *Niall P. Kelly*[1,3], *Ludovic Caro*[1,3], *Frank H. Peters*[1,3]
[1]*Integrated Photonics Group, Tyndall National Institute, Dyke Parade, Cork, Ireland*
[2]*Electrical and Electronic Engineering Department, University College Cork, College Road, Cork, Ireland*
[3]*Physics Department, University College Cork, College Road, Cork, Ireland*
✉ *E-mail: mohamad.dernaika@tyndall.ie*

Abstract: A single mode laser based on coupled cavities of an active ring laser and a Fabry Perot is presented. The laser exhibits tunable single mode behaviour with a side mode suppression ratio of 41 dB and a line-width of 400 kHz.

1 Introduction

Regrowth-free semiconductor lasers have attracted considerable interest due to their relatively simple fabrication. In addition, similar to Bragg based lasers they offer a stable single longitudinal mode with the advantage of wide tuning without additional fabrication complexity by employing thermal and Vernier tuning mechanisms. Examples of such designs include coupled cavity lasers that rely on the coupling of multiple resonating cavities with different free spectral ranges (FSR) to achieve single mode operation [1–4]. These laser designs provide a high side mode suppression ratio (SMSR) that exceeds 40 dB, tunable output across the C + L band and narrow line-width without the need of an external cavity or high-resolution lithography as required by distributed Bragg reflector and distributed feedback lasers [5, 6].

Microring lasers have been extensively investigated as filters and they are considered a promising optical component due to their superior filtering characteristics, serving as an excellent wavelength selective element [7–9]. Due to their facet-less operation they can be monolithically integrated with other devices [10–13]. Using standard ultraviolet (UV) lithography various coupling techniques can be used to couple light between the ring and the waveguide, such as multimode interference couplers [14–16], Y-junctions [17], directional couplers [18, 19] and half wave couplers (HWCs) [20–22]. HWCs offer the advantage of compactness, coupling ratio flexibility and high fabrication tolerance, making them ideal to fabricate high yield rings with a large FSR to improve the laser SMSR in active InP based material using standard photolithography.

In this study, we demonstrate a tunable single mode laser based on coupled cavities between a ring and a Fabry Perot (FP) laser. The coupled laser achieved a narrow line-width of 400 kHz and an SMSR of 41 dB. The laser is tunable across 24 nm over five discrete channels that are 6 nm apart.

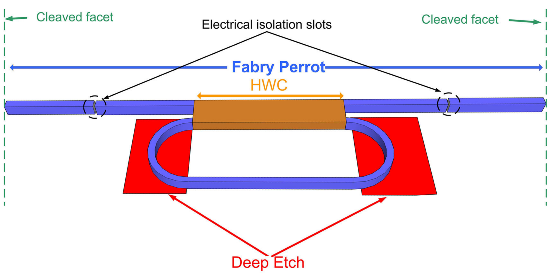

Fig. 1 *Illustration of the laser cavity design showing the FP and ring cavity*

2 Laser design and fabrication

Fig. 1 shows an illustration of the laser cavity design. The cavity consist of a 1000 μm long FP laser and a ring laser coupled via a 90 μm × 6 μm (length × width) HWC. The red area in Fig. 1 represents the deep etch region used to increase the optical mode confinement to reduce the loss at the bends. The effective ring radius was chosen to be 50 μm to reduce the ring size and maintain a relatively large FSR. Moreover, the ring bends were designed to be trapezoidal in order to further reduce the bending loss. More detailed information about the bends' characteristics and optimization can be found in [23, 24]. The cavity is divided into three sections via two angled isolation slots as shown in Fig. 1 to improve the wavelength tuning and optimise the SMSR. The HWC was designed and optimised using the commercial software BeamPROP from RSoft. The splitting ratio of the coupler is 10:80, in which 80% of the light is cross coupled and 10% is straight coupled.

The simulation of the HWC is shown Fig. 2*a* where a power monitor shows the evolution of coupling along the length of the coupler. The green line and blue line represent the cross and the direct coupling, respectively. The observed residual loss of around 10% can be optimised by increasing the length and width of the coupler. However, this size increase will consequently reduce the longitudinal mode spacing which can limit the SMSR of the laser. A series of cavities using various coupler lengths and widths were fabricated and tested, with the 90 μm × 6 ×μm HWC showing the highest SMSR. The reported HWC was also optimised to be compatible with UV contact lithography with a width of 6 μm and an input/output waveguide width of 2.5 μm spaced at 1 μm. Fig. 2*b* shows the mode field shape, diameter and intensity just at the HWC outputs for cross and direct coupling. The cross-coupling power is visibly stronger as expected from 80:10 coupling ratio. Fig. 2*c* shows the illustration of the HWC with its dimension along with the direct and cross outputs. A microscopy and scanning electron microscopy (SEM) image of the cavity and the coupler are shown in Fig. 3.

Fig. 3*a* shows a microscopy image of the three-section laser cavity. Three separate metal pads were used to bias the laser. The sections are isolated using a 7°, 1 μm wide angled shallow slot (1.75 μm deep) etched to just above the active region to minimise reflections (Fig. 3*b*). The laser was fabricated using a regrowth-free and standard UV lithography process using commercial off the shelf multiple quantum well International Quantum Epitaxy (IQE) material. The epitaxial layers were grown on an n-doped InP substrate using 5 × 6 nm strained quantum wells with 10 × 6 nm barriers. The process consisted of two etch depths: shallow and deep. The shallow etch depth of 1.78 μm was used to define the

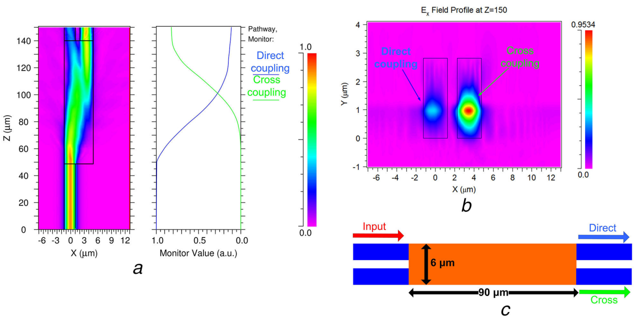

Fig. 2 *80 : 10 half wave coupler simulation and design*
(a) Simulation of the HWC showing the direct and cross power coupling ratios, ***(b)*** Modes' intensity at the two output waveguides, ***(c)*** Illustration showing HWC dimensions and outputs

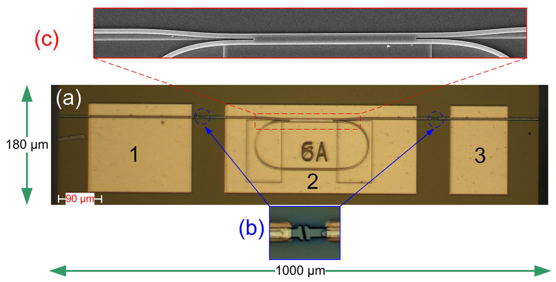

Fig. 3 *Microscope and SEM images of the laser cavity*
(a) Microscopy image of the laser cavity, ***(b)*** Close up image of the isolation slot, ***(c)*** SEM image of the HWC

ridges, isolation slots and HWC. The deep etch region was only used for the ring bends as shown in Fig. 1. Moreover, the P and N metal depositions were as follows: 20:400 nm Ti:Au P-metal and 20:250 nm Ti:Au back side metal. Finally, the substrate was thinned from 350 to 100 μm using bromine methanol.

3 Results and discussion

The laser was mounted on a temperature controlled brass chuck with a fixed temperature of 15°C. A lensed fibre at one of the cleaved facets was used to collect the light. At the lensed fibre output, a power meter and an optical spectrum analyser were used to measure the laser power and spectrum, respectively.

To test the ring coupled HWC operation and to ensure it is lasing solely without the need of cleaved facets, the ring pad 2 (Fig. 3*a*) was biased at 100 mA, whereas pad 1 was set at a reverse bias of −3 V to act as a light absorber to eliminate any interaction with the left cleaved facet. Pad 3 was then left unbiased to couple the light out into a lensed fibre. The optical spectrum taken using an Ando AQ6317 optical spectrum analyser (resolution of 0.01 nm) is shown in Fig. 4.

Fig. 4 show the spectrum collected from the right facet while only the ring pad is biased. The inset figure shows that the FSR is 1.2 nm which corresponds to ring cavity length. The lasing threshold of the ring was measured at ∼70 mA, and this high lasing threshold is due to the low Q of the ring caused by the 80% cross coupling of the HWC. It is worth noting that the deep to shallow transitions were measured in separate FP structures, where no modulation in the optical spectra was seen. Thus, any reflections from these transitions are negligible in their effect on the optical spectra.

Fig. 5*a* shows the laser spectrum with an SMSR of 41 dB with all three pads biased. Moreover, Fig. 5*b* shows the laser light-intensity (L-I) plot with a lasing threshold of around 24 mA. The L-I plot measurement was taken by biasing pads 1 and 3 as shown in Fig. 3*a* at 15 mA each and sweeping the current applied to the ring (pad 2) from 0 to 60 mA.

Taking in consideration that the laser cavity is active: the low (10%) through coupling in the ring is easily compensated by the gain in the ring, such that the ring is able to lase on its own (as seen in Fig. 4). At, or near this lasing condition, the ring acts as a very

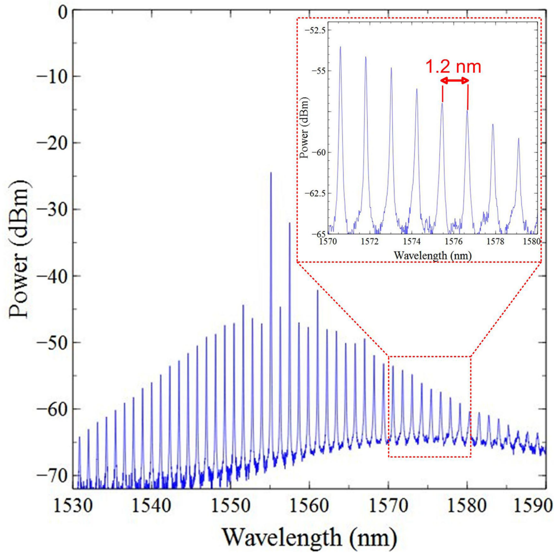

Fig. 4 *Spectrum with only ring pad is biased (at 70 mA), inset showing ring FSR*

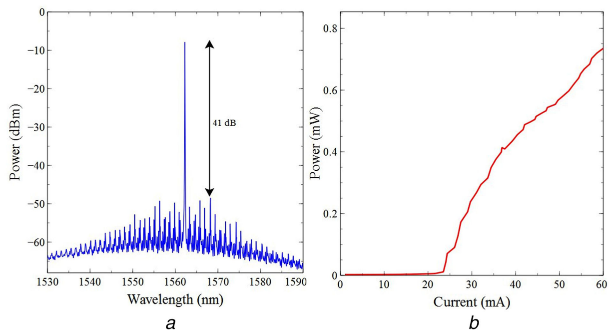

Fig. 5 *Single mode operation of the laser and its output power performance*
(a) Single mode with a SMSR of 41 dB (ring biased at 100 mA, Pad 1 and Pad 2 at 10 mA), ***(b)*** L-I plot of the laser cavity

strong high-Q mode filter acting on the FP portion of the laser, while providing significant gain at the resonant condition. This strong filtering is made possible due to gain in the ring. For passive filters, a high through coupling is required to enable a good filter, and this design is therefore more often used. Such a design, with a higher though coupling, would still result in a good mode filter, but would provide significantly less gain for the laser. Thus, our choice of coupler (low through coupling and high cross coupling) utilises both the filtering and gain properties of the ring section resulting in a better compound laser with better SMSR than the opposite coupler (high through coupling and low cross coupling). The concept of controlling the Q cavity of an active ring by increasing the gain has been studied and demonstrated in active–passive waveguides such as in [12], where an semiconductor optical amplifier (SOA) was used to compensate the loss of the ring, drastically increase the Q-factor and enhance the filter capabilities of the ring.

Fig. 6 shows the 400 kHz measured line-width (blue dots) and its Lorentzian fit (red line) of the single mode, shown in Fig. 5*a*.

The laser line-width was measured using a delayed self-heterodyne, recirculating loop technique reported in [25] using a 50 km fibre delay line. This technique has a resolution accuracy < 2 kHz, and the experimental setup can be found in [26].

The cavity can be tuned over 24 nm by changing the injection current, achieving five tunable channels with 6 nm spacing. Fig. 7*a* shows the overlap spectrum of the various wavelengths extending from 1555 to 1584 nm. The performance of the individual channels in terms of SMSR and power can be seen in Fig. 7*b*. The laser achieves a good SMSR across all channels that vary between 34 and 41 dB. Moreover, power up to 2.5 mW was coupled via the lensed fibre, with most channels having > 1 mW output. It is

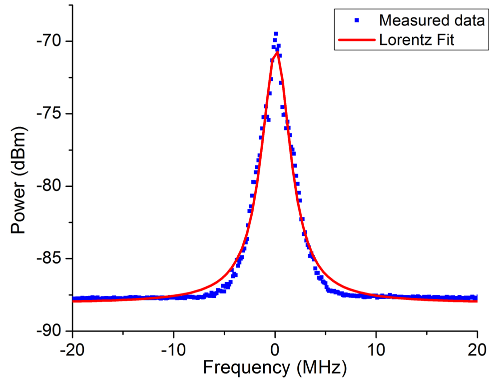

Fig. 6 *Measured 400 kHz laser line-width (blue dots) of the spectrum in Fig.5 with same operation conditions, and the corresponding Lorentzian fit (red line)*

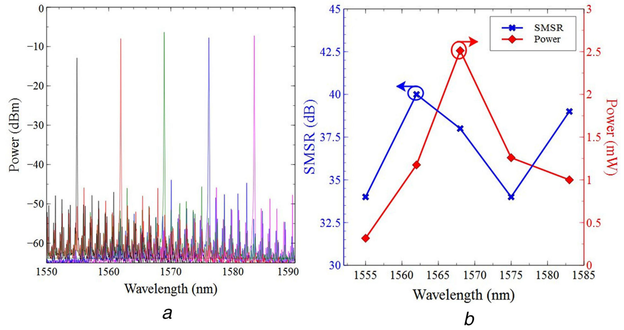

Fig. 7 *Tunable channels with their relevant SMSR and optical power*
(a) Laser tunability across five channels, ***(b)*** Power and SMSR performance for each of the channels

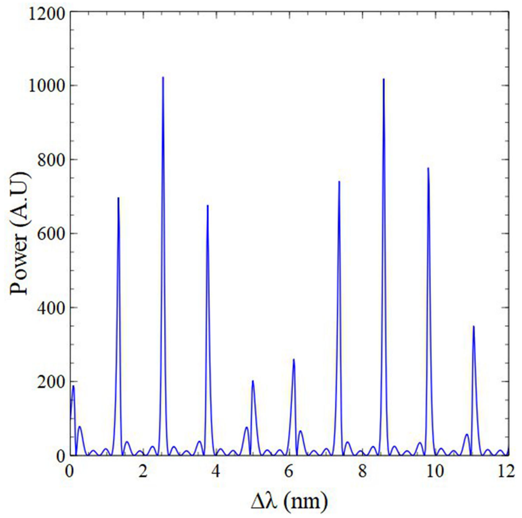

Fig. 8 *Simulation of the compound laser resonance of the ring and FP cavities, with 6 nm spacing between main peaks*

important to mention that to simplify the overall laser fabrication and processing no high reflection coating was used on any of the facets. Fig. 8 shows the simulated, near threshold spectrum of the laser with relevant spacing. The 6 nm FSR of the compound laser is caused by the resonance between the ring and the FP sections of the laser.

The compound semiconductor laser presented have the advantage of combining a relatively small foot print and a sub-MHz line-width. In comparison with similar designs, the presented laser covers a wide tuning range across 24 nm, whereas the cavities in [3, 22] for example offer a finer tuning over a few nanometres. Other designs, such the slotted FP cavities have a narrow line-width that can reach tens of kHz and wide tuning range, however these laser cavities can extend over 2 mm in length.

4 Conclusion

This study demonstrates a regrowth-free semiconductor laser based on coupled cavities of a FP and a ring laser via a HWC. The cavity exhibited a single mode operation with an SMSR of 41 dB and a line-width of 400 kHz without the need of optical coating or complicated design. The power and SMSR performance of the various tunable channels was also presented.

5 Acknowledgment

This work was supported by the Science Foundation Ireland under grants SFI 13/IA/1960 and 12/RC/2276 (I-PIC).

6 References

[1] Morrissey, P.E., Kelly, N., Dernaika, M., *et al.*: 'Coupled cavity single-mode laser based on regrowth-free integrated mmi reflectors', *IEEE Photonics Technol. Lett.*, 2016, **128**, (12), pp. 1313–1316

[2] Kelly, N.P., Dernaika, M., Caro, L., *et al.*: 'Regrowth-free single mode laser based on dual port multimode interference reflector', *IEEE Photonics Technol. Lett.*, 2017, **29**, (3), pp. 279–282

[3] Wang, Y., Yang, Y., Zhang, S., *et al.*: 'Narrow linewidth single-mode slotted Fabry–Pérot laser using deep etched trenches', *IEEE Photonics Technol. Lett.*, 2012, **24**, (14), pp. 1233–1235

[4] Byrne, D.C., Engelstaedter, J.P., Guo, W.H., *et al.*: 'Discretely tunable semiconductor lasers suitable for photonic integration', *IEEE J. Sel. Top. Quantum Electron.*, 2009, **15**, (3), pp. 482–487

[5] Komljenovic, T., Srinivasan, S., Norberg, E., *et al.*: 'Widely tunable narrow-linewidth monolithically integrated external-cavity semiconductor lasers', *IEEE J. Sel. Top. Quantum Electron.*, 2015, **21**, (6), pp. 214–222

[6] Lewoczko-Adamczyk, W., Pyrlik, C., Häger, J., *et al.*: 'Ultra-narrow linewidth DFB-laser with optical feedback from a monolithic confocal Fabry–Perot cavity', *Opt. Express*, 2015, **23**, (8), pp. 9705–9709

[7] Hamacher, M., Troppenz, U., Heidrich, H., *et al.*: 'Active ring resonators based on GaInAsP/InP'. Proc. Photonics Fabrication Europe, Bruges, Belgium, 2002, (SPIE, 4947), pp. 212–222

[8] Matsuo, S., Segawa, T.: 'Microring-resonator-based widely tunable lasers', *IEEE J. Sel. Top. Quantum Electron.*, 2009, **15**, (3), pp. 545–554

[9] Grover, R., Van, V., Ibrahim, T., *et al.*: 'Parallel-cascaded semiconductor microring resonators for high-order and wide-FSR filters', *J. Lightwave Technol.*, 2002, **20**, (5), p. 872

[10] Segawa, T., Matsuo, S., Kakitsuka, T., *et al.*: 'Monolithically integrated filter-free wavelength converter with widely tunable double-ring resonator coupled laser'. 20th Int. Conf. on Indium Phosphide and Related Materials, 2008 (IPRM 2008), 2008, pp. 1–4

[11] Furst, S., Yu, S., Sorel, M.: 'Fast and digitally wavelength-tunable semiconductor ring laser using a monolithically integrated distributed Bragg reflector', *IEEE Photonics Technol. Lett.*, 2008, **20**, (23), pp. 1926–1928

[12] Rabus, D.G., Hamacher, M., Troppenz, U., *et al.*: 'Optical filters based on ring resonators with integrated semiconductor optical amplifiers in GaInAsP-InP', *IEEE J. Sel. Top. Quantum Electron.*, 2002, **8**, (6), pp. 1405–1411

[13] Kapsalis, A., Stamataki, I., Mikroulis, S., *et al.*: 'Widely tunable all-active microring lasers', *IEEE Photonics Technol. Lett.*, 2006, **18**, (24), pp. 2641–2643

[14] Pennings, E., van Roijen, R., van Stralen, M., *et al.*: 'Spectral behavior of InP-based ring lasers employing multimode interference devices'. Lasers and Electro-Optics Society Annual Meeting, 1993. LEOS'93 Conf. Proc. IEEE, 1993, pp. 617–618

[15] Rabus, D.G., Hamacher, M.: 'MMI-coupled ring resonators in GaInAsP-InP', *IEEE Photonics Technol. Lett.*, 2001, **13**, (8), pp. 812–814

[16] Kim, S., Byun, Y.T., Kim, D.G., *et al.*: 'Fabrication of coupled-ring reflector laser diodes consisted of total internal reflection mirrors and multimode interference coupler'. Int. Conf. on Photonics in Switching, 2008 (PS 2008), 2008, pp. 1–2

[17] Sun, Y., Shih, M.: 'A circular ring laser diode with tow Y-junction couplers'. 2012 21st Annual Wireless and Optical Communications Conf. (WOCC), 2012, pp. 206–208

[18] Suzuki, S., Oda, K., Hibino, Y.: 'Integrated-optic double-ring resonators with a wide free spectral range of 100 GHz', *J. Lightwave Technol.*, 1995, **13**, (8), pp. 1766–1771

[19] Rabus, D.G., Bian, Z., Shakouri, A.: 'A GaInAsP-InP double-ring resonator coupled laser', *IEEE Photonics Technol. Lett.*, 2005, **17**, (9), pp. 1770–1772

[20] Lin, X., Liu, D., He, J.J.: 'Design and analysis of 2×2 half-wave waveguide couplers', *Appl. Opt.*, 2009, **48**, (25), pp. F18–F23

[21] He, J.J., Liu, D.: 'Wavelength switchable semiconductor laser using half-wave V-coupled cavities', *Opt. Express*, 2008, **16**, (6), pp. 3896–3911

[22] Wu, L., Wang, Y., Yu, T., *et al.*: 'Wavelength switchable semiconductor laser based on half-wave coupled Fabry–Pérot and rectangular ring resonators', *IEEE Photonics Technol. Lett.*, 2012, **24**, (12), pp. 991–993

[23] Sheehan, R.N., Horne, S., Peters, F.H.: 'The design of low-loss curved waveguides', *Opt. Quantum Electron.*, 2008, **40**, (14–15), pp. 1211–1218

[24] Sheehan, R.N., Peters, F.H.: 'Bends in the plane with variable curvature', *Math. Soc. Bull.*, 2016, **78**, (Winter 2016), pp. 61–80

[25] Tsuchida, H.: 'Simple technique for improving the resolution of the delayed self-heterodyne method', *Opt. Lett.*, 1990, **15**, (11), pp. 640–642

[26] Alexander, J., Morrissey, P., Yang, H., *et al.*: 'Monolithically integrated low linewidth comb source using gain switched slotted Fabry–Perot lasers', *Opt. Express*, 2016, **24**, (8), pp. 7960–7965